Preferred citation: H. Corte. The porous structure of paper – Its measurement, its importance and its modification by beating. In **Fundamentals of Papermaking Fibres**, *Trans. of the Ist Fund. Res. Symp. Cambridge, 1957*, (F. Bolam, ed.), pp 301–331, FRC, Manchester, 2018. DOI: 10.15376/frc.1957.1.301.

THE POROUS STRUCTURE OF PAPER

ITS MEASUREMENT, ITS IMPORTANCE AND ITS MODIFICATION BY BEATING

H. CORTE

PHYSICAL CHEMISTRY INSTITUTE, UNIVERSITY OF GÖTTINGEN, GERMANY

Abstract

In order to treat the porosity properties of paper from a common viewpoint, its porous structure is described by means of the pore size distribution. Two methods for its determination are discussed in detail. A general result, supported by statistical considerations, is that the frequency distribution of the pore radii can be approximated by a logarithmic Gauss distribution. Over a wide range of porosity, simple linear relationships between the characteristic parameters of the distributions were found.

Considering the various possible permeation phenomena, the permeation of inert gases (such as air) is the simplest case. It is governed by the Poiseuille law at normal pressures. At low pressures, the Knudsen and the slip effect come into play. Permeation of water vapour is shown to be a surface diffusion process, additionally controlled by the adsorption of water vapour on cellulose. This process, including its temperature dependence, can be reduced to air permeability and water vapour adsorption. The penetration of inert liquids follows the Poiseuille law, but is affected additionally by the interface tension between the liquid and cellulose. The quantitative treatment reveals a relationship between the leak time of such liquids (as grease) and the air permeability, which has been proved by experiments.

Introduction

THE porous structure of paper is one of its fundamental qualities. Many applications of paper are based on it (filter paper, blotting paper, sanitary papers). In other cases, the practical value of paper is limited by its porosity and considerable efforts are made to diminish it. The spreading of ink is hindered by sizing; impregnation with paraffin wax or lamination with plastics make the paper less permeable to water vapour or even make it water repellent. On the whole, there are many applications that are, in one or the other sense, affected by porosity. Consequently, there exist many specifications and paper tests concerning single porous properties.

Similar to the large group of mechanical paper tests, most of the test methods for porosity, too, are fitted to some special case of application. They are often of only little value for general information. Furthermore, for some special properties, there exist several test methods — for example, there may be 20—25 methods for the sizing test and also many methods for testing grease resistance. The large number of porosity tests has not always contributed to the enlargement of our knowledge, but has often led to confusion. Nowadays, the problems of papermaking and paper testing are dealt with in a more and more scientific manner. Consequently, we feel the need for systematic exploration of the various processes. In the field of mechanical paper properties, important results have already been brought about. In the field of porosity phenomena, we can try to reduce the mass of phenomena to as few physical laws as possible, in order to describe them as economically as possible.

By porosity phenomena, we understand here those phenomena connected with the penetration of matter into paper or the permeation of matter through paper. It should be possible to describe all these phenomena from a common viewpoint, if we know —

1. The geometrical porous structure of paper;
2. The interaction between the penetrating or permeating matter and cellulose;
3. The transport equations and the other physico-chemical laws that have to be applied in the individual cases.

Porous structure

To begin with the porous structure, we describe it by means of the pore radius distribution. It is quite clear that the real structure of a paper sheet can only be revealed by optical inspection and can only be described in many words. At the present time, it is not possible to characterise porous structure numerically in such a manner that anybody receives a clear impression of a

sheet of paper by these figures. Consequently, it is necessary to use a model. For our present purpose, the kind of model is not very important. We know that the concept of a pore radius is a physical fiction. It originates from transferring physical laws valid for annular pores to the structure of paper.

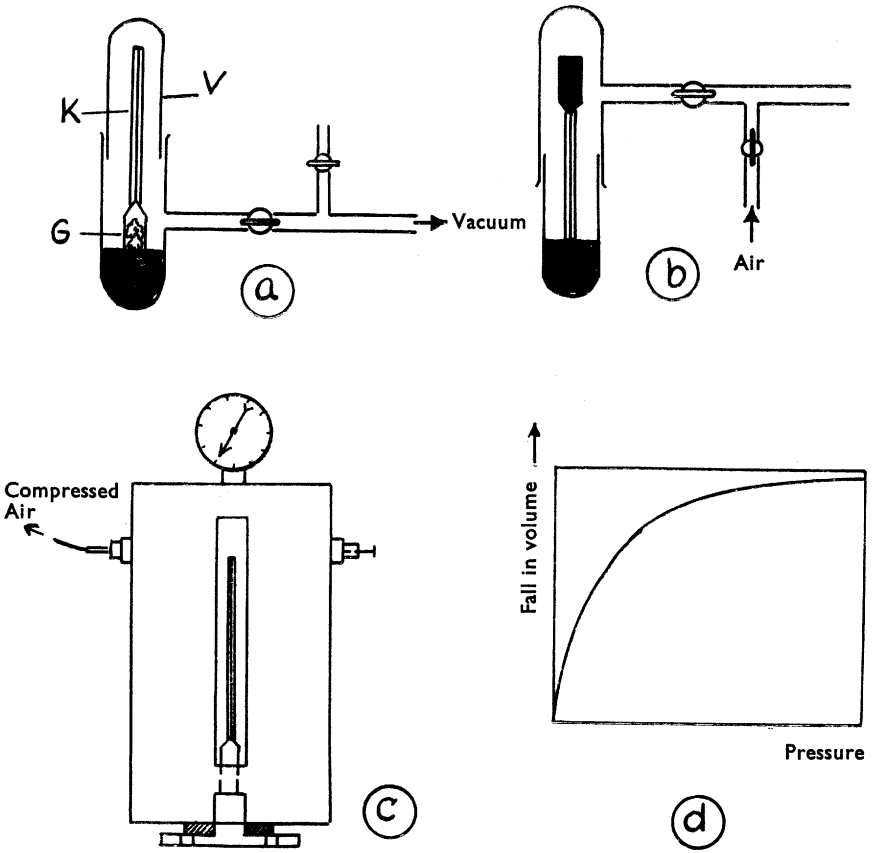

Fig. 1 — Determination of the pore size distribution by volume (after Wakeham)

It is possible to transform these laws or equations into other forms, using other concepts, such as specific surface or free pore volume. In this way, the Poiseuille equation can be transformed into, for example, the Kozeny equation. But, to be exact, the properties and terms in more generalised

equations also are physical fictions. They appear as the results of certain experiments if they are evaluated according to a certain mathematical operation. It does not matter what kind of model is used, provided the experimental results as interpreted by the model are in accord. We will therefore use the simplest model, using the concept of definite pore radii.

There are several methods of determining the pore radius distribution, of which two may be mentioned here. One of them has been described by Wakeham. The principle can be seen in Fig. 1. The sample (about 0.3 g.) is enclosed in a glass bulb *G* (*a*). The glass bulb is fitted with a capillary tube some 20 cm. long (*K*) and is placed in a wider tube *V*. The wider tube contains a certain amount of mercury. The whole assembly is evacuated for some hours by means of a high vacuum pump. After evacuation, the apparatus is turned through 180°, separated from the pump and opened to the air. The mercury penetrates through the capillary tube into the glass bulb, filling all larger pores and the smaller ones down to about 10^{-3} cm. radius (*b*). Now the bulb is transferred into a steel housing (*c*), which is connected to a source of compressed air. If the pressure is raised stepwise, the mercury will be forced into smaller and smaller pores. The volume of mercury disappearing at each pressure step is obtained from the drop in the meniscus in the capillary. Correction has to be made for the compressibility of mercury by performing the same experiment without a paper sample. The radius of pores entered at each pressure step can be calculated from the pressure, p and the surface tension of mercury, σ, according to the Kelvin equation —

$$p = \frac{2\sigma}{r}\cos\theta = -\frac{2\sigma^*}{r} \quad \ldots\ldots\ldots\ldots\ldots\ldots \quad (1)$$

where r is the pore radius and θ the contact angle, which is here 180° ($\cos\theta = -1$). A plot of the volume, v, of mercury disappearing into the pores against the pressure has the form of graph (*d*) in Fig. 1. Further evaluation is based on equation (*1*) —

$$\frac{dv}{dr} = \frac{dv}{dp}\,\frac{dp}{dr} = \frac{2\sigma}{r^2}\,\frac{dv}{dp} = \frac{1}{2\sigma}p^2\frac{dv}{dp} \quad \ldots\ldots\ldots\ldots \quad (2)$$

A plot of $\frac{1}{2\sigma}\,p^2\,\frac{dv}{dp}$ against $r = -\frac{2\sigma}{p}$ gives the pore size distribution by volume.

The area under the curve corresponds to the whole volume in the sample.

Fig. 2 and 3 show some typical results, exhibiting the influence of beating time and machine glazing, respectively, on the pore size distribution.

* The negative sign means that the hydrostatic pressure is directed into the pores

An interesting detail can be seen in Fig. 2, as a mixture of a free beaten and a wet beaten pulp gives two maxima at pore radii of the single pulp maxima.

Three experimental details —

1. The temperature must be kept carefully constant, as the mercury-filled glass bulb is a sensitive thermometer.
2. Curves for rising and falling pressure often show hysteresis due to the compressibility of the fibres. A certain time after each pressure step is required to establish hydrostatic equilibrium and to avoid hysteresis.
3. It is difficult to obtain closed distribution curves. Observation at pressures well below atmospheric pressure may close the right branch of the curve, but, to close the left branch, very high pressures are necessary. It is hardly possible therefore to get the frequency curve by number out of the frequency curve by volume.

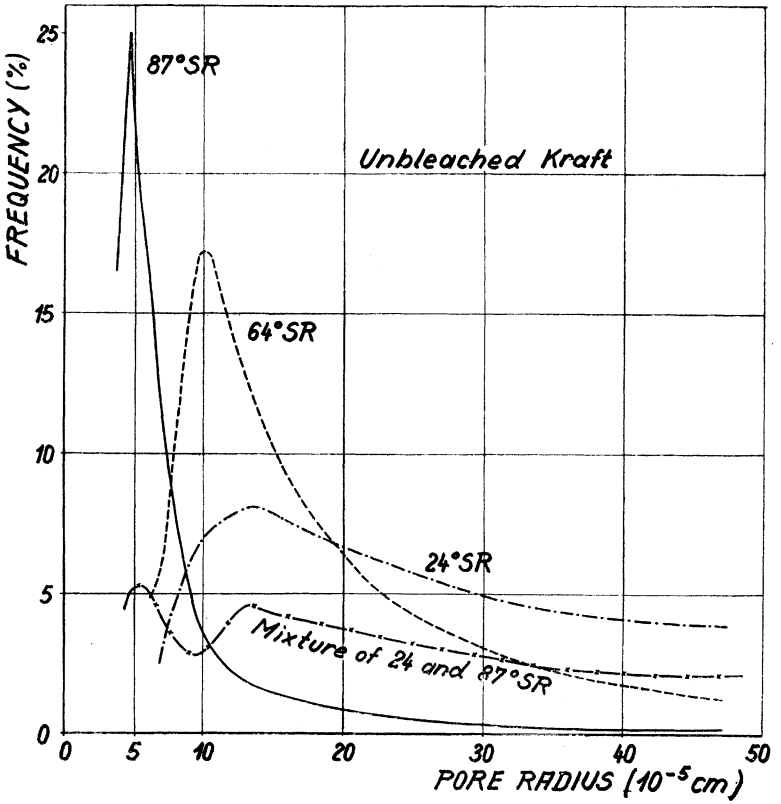

Fig. 2 — Pore size distribution of papers from different beaten pulps

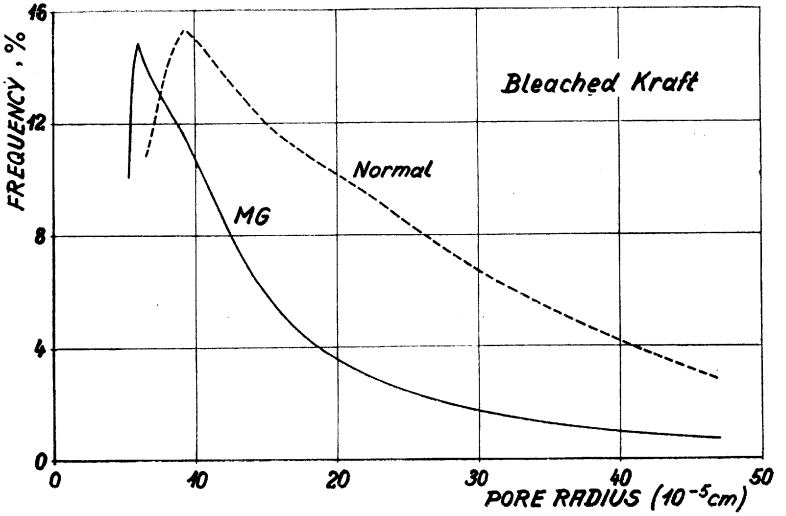

Fig. 3 — Effect of machine glazing on the pore size distribution

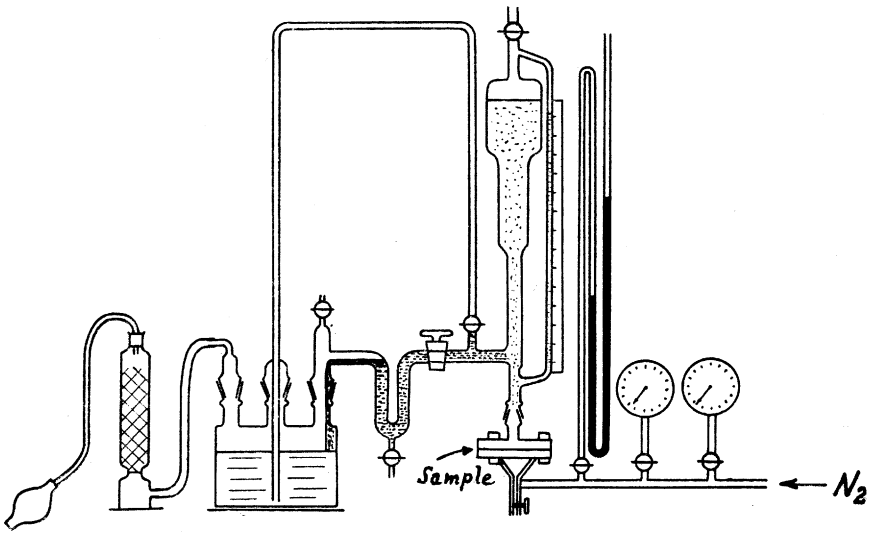

Fig. 4 — Determination of pore size distribution by area or by number (dioxane method)

The latter disadvantage can be overcome by the second method. The principle is shown in Fig. 4. Instead of observing the stepwise penetration of a liquid into the pores (method *1*), we now observe the stepwise permeation of a gas through the pores. The sample is clamped between metal rings, fitted with screens and covered by a liquid that does not swell the cellulose (such as dioxane). The dioxane fills a tube above the sample and the whole assembly is closed against atmospheric moisture. Nitrogen is used to exert

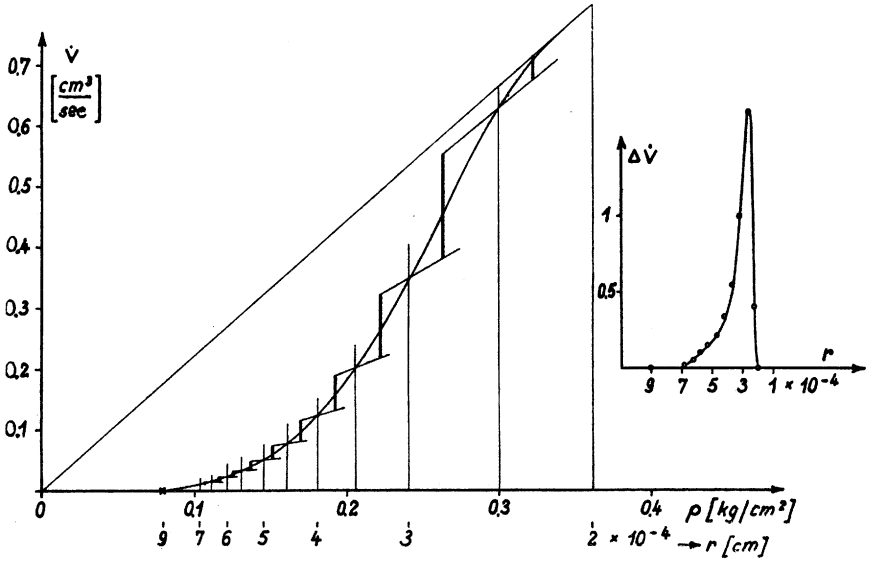

Fig. 5 — Evaluation of rate of flow/pressure curve from the dioxane method

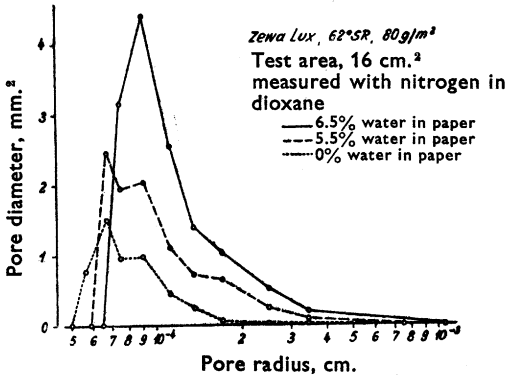

Fig. 6 — Pore size distribution of paper with various water contents

pressure against the paper sheet from below. At a certain pressure, the first bubbles come out of the paper, having passed through the largest pores. The radius of these pores can also be calculated from equation (*1*), the contact angle θ being zero and the hydrostatic pressure having the opposite sign as in the mercury method.

When the pressure is raised, the velocity of flow would be proportional to the pressure if no other pores were opened. In fact, the rising pressure opens more and more of the smaller pores, according to the Kelvin equation. Consequently, the flow rate increase is more than proportional to the pressure.

The measuring tube is divided into sections of different diameter to provide for different flow rates. In addition, different manometers can be used for different pressure ranges.

A typical plot of the flow velocity against pressure is shown in Fig. 5. Because of the low surface tension of dioxane, very small pores can be entered at reasonable pressures and, in many cases, the curve approximates to the Poiseuille straight line through the origin, when no further pores are opened. In this case, the distribution curve is closed. The experimental curve can be evaluated graphically as shown in Fig. 5. The rise in flow rate at each pressure step can be transformed, applying the Poiseuille law, into the area or number of pores with a radius belonging to this pressure step.

Fig. 6 shows results of measurements in which small amounts of water had been added to the dioxane. In separate experiments, the distribution equilibrium of water between dioxane and cellulose had been checked. The graph shows the typical effect of water content on the porosity of the paper sample.

A special advantage of this method is the possibility of detecting irregularities in the porous texture of the paper sheet. Fig. 7 shows measurements on a greaseproof paper compared with those on vegetable parchment. The latter is less porous on the whole, but it shows a second maximum at rather large pore sizes (in most cases, this small maximum was found far more to the right), indicating pinholes, which seemed to be typical for the production process of this material.

The two methods described here represent distinctly different experiments. The results cannot be compared in detail, but only qualitatively. In Fig. 8 are shown results on the same sample of paper, using both methods (the scales of the ordinates were chosen to give nearly equal heights to the maxima). As the mercury method gives the distribution by volume and the volume is proportional to the second or third power of the pore radius, the

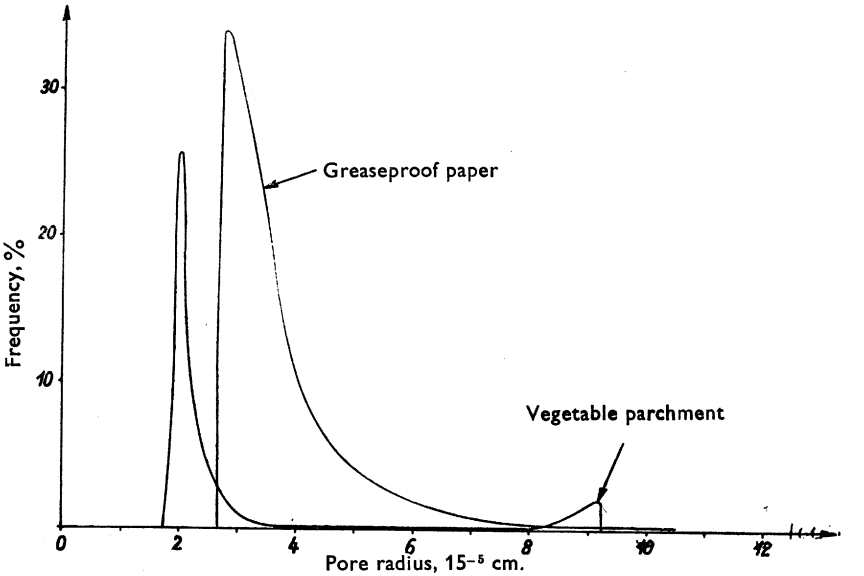

Fig. 7 — Pore size distribution of vegetable parchment compared with greaseproof paper

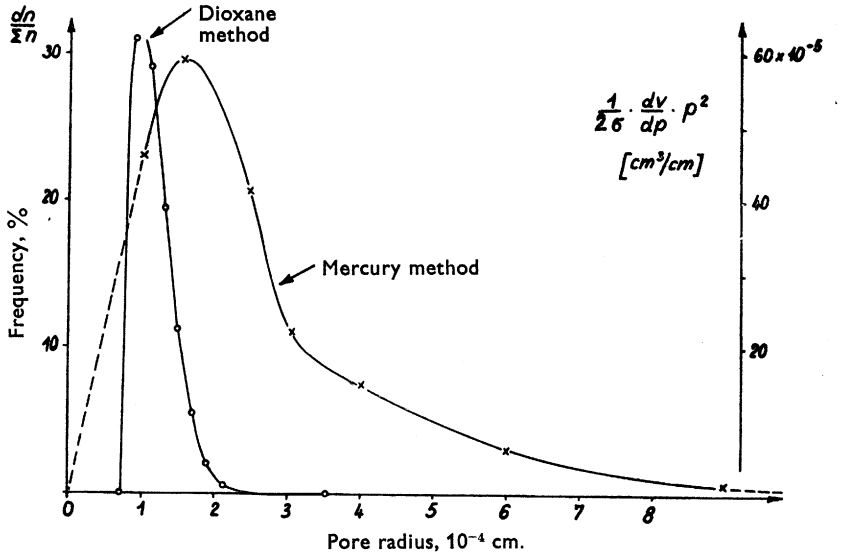

Fig. 8 — Comparison of the dioxane and mercury methods

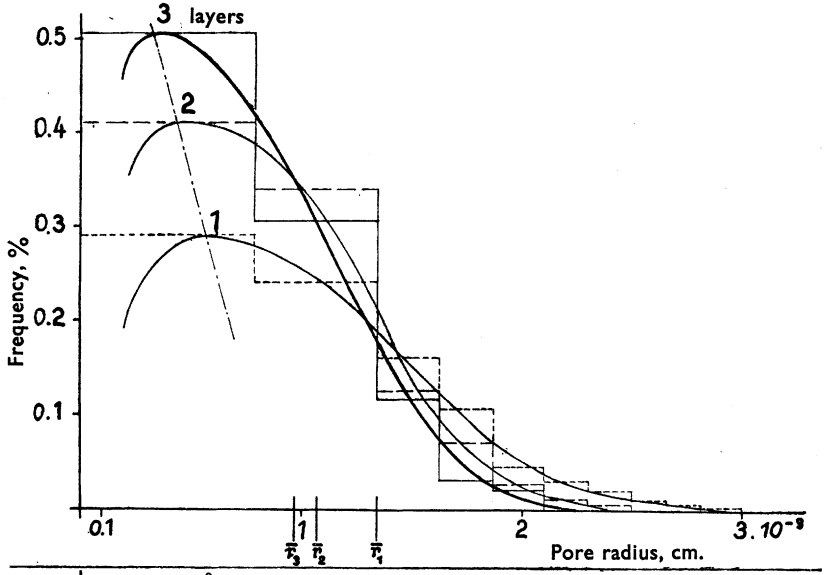

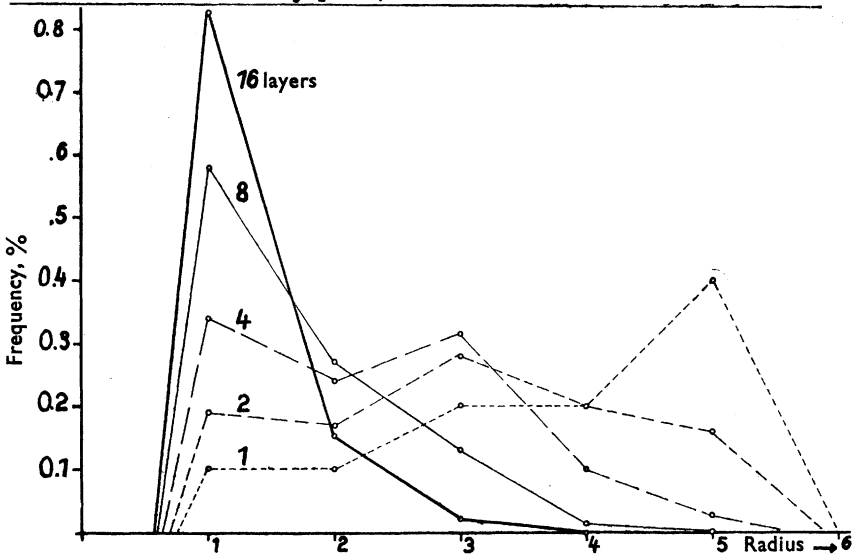

Fig. 9 (*above*) — Pore size distribution of thin layers of paper (measured optically)

Fig. 10 — Calculated variation of pore size distribution by combination of single layers

maximum of this curve is displaced towards higher pore radii compared with the distribution curve by number obtained by the dioxane method.

Both curves have an unsymmetrical shape and both methods give pore radii of 10^{-4} — 10^{-5} cm.

The next step is to describe the distribution curve (by number) analytically. Experiments have shown that the frequency distribution can be fitted by a logarithmic Gauss distribution — that is, a normal Gauss distribution for the logarithm of the pore radius. Such a form could be supported by theoretical considerations based on statistics.

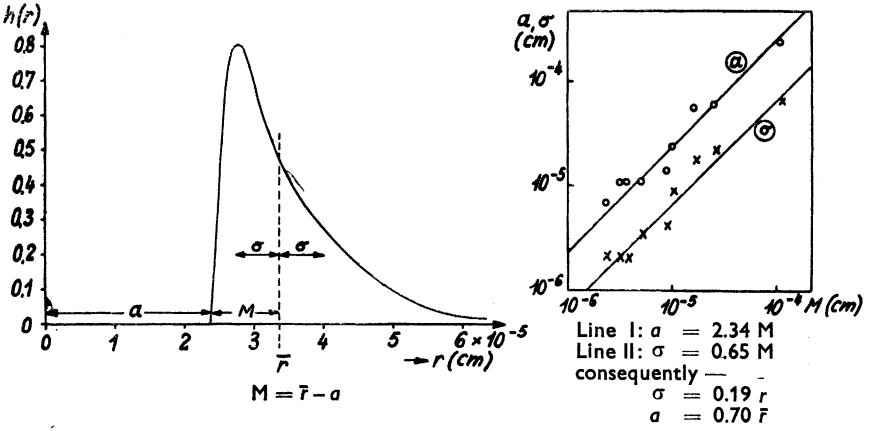

Fig. 11 — Two rules for the logarithmic pore size distribution

Experiments have been made with layers of very thin sheets. Contact photographs were taken and the optically open holes were measured. Fig. 9 shows the results for a series of 1, 2 and 3 layers. The distribution approximates to a logarithmic Gauss curve. Statistical treatment has been made, considering a paper sheet as consisting of a number of layers with an arbitrary hole size distribution. Calculating the probability of finding a hole of a certain size at a given place, the hole size distribution for sheets of 2, 3, etc. layers can be found. The calculation (not given here) shows that, with an increasing number of layers, a logarithmic Gauss distribution is approximated to whatever the hole size distribution of the single layer is like. Fig. 10 shows the result of such a calculation. An arbitrary distribution with a maximum at radius 5 is supposed for each single layer. It can be seen that the maximum shifts to the left and that with 16 layers a logarithmic Gauss distribution is very well approximated.

Fig. 11 shows such a distribution. It is determined by the (extrapolated) smallest value a, the mean value $\bar{r}$ and the variation σ. A comparison of various papers showed (over a range of two powers of ten in the mean pore radius) linear relationships between these parameters. They are given in the diagram Fig. 11. According to these relationships, the width of the curve increases linearly with the mean pore radius. We do not know, at present, the cause for this behaviour, but we will see a practical consequence of it later on.

Permeation

Permeation phenomena can be classified, according to physical and practical aspects, as shown in Table 1.

TABLE 1

Classification of permeation phenomena

		Permeating material	
		Gas	*Liquid*
Interaction with the pore walls	*No*	Air (cement bags)	Grease, printing ink (glassine, printing paper)
	Yes	Water vapour (moistureproof papers)	Water (writing, tissues, etc.)

All the four cases have practical importance. Mixtures between the classes are possible, such as permeation of moist air and moist grease (for example, butter). Laminated and multilayer materials show further complications.

Air

The simplest case is the permeation of dry air through paper. We should expect a generalised form of the Poiseuille law to be valid, that is, that the rate of flow (volume) is proportional to the pressure drop. When the mean pressure is varied, the rate of flow is better expressed in c.c. at S.T.P. per unit time. This reduced volume is proportional to the pressure. So we have —

$$\dot{v} \text{ is proportional to } \bar{p}\ \Delta p,$$

where $\dot{v}$ is the flow rate (volume at S.T.P. per unit time and unit area), $\bar{p}$ the mean pressure and Δp the pressure drop. A suitable apparatus for making these measurements is shown in Fig. 12. The paper membrane closes a glass shell, which is fixed in a larger shell S. Both shells are connected by a differen-

tial manometer *D*, filled with liquid paraffin, indicating the pressure drop. The shells can be connected with containers *I* and *II* or with a small glass bulb *V* containing water. The whole apparatus can be evacuated, the manometer *M* indicating the absolute pressure. Shell *S* is put into a thermostatically controlled bath.

After evacuation, the whole apparatus is filled with dry air up to a certain pressure, equal on both sides of the paper membrane. Now the pressure on one side of the paper is raised by a small amount, say, 1 mm. mercury. The pressure difference will fall owing to the permeation of air and its course can be followed by the differential manometer. The permeation rate is given by equation (*4*) —

$$\frac{\dot{n}}{\Delta p} = -\frac{v_I\, v_{II}}{v_I+v_{II}} \cdot \frac{1}{RT} \cdot \frac{1}{\Delta p} \cdot \frac{d(\Delta p)}{dt} = -\frac{v_I\, v_{II}}{v_I+v_{II}} \cdot \frac{1}{RT} \cdot \frac{d\,\ln(\Delta p)}{dt} \quad \ldots\ldots\ldots (4)$$

where $\dot{n}$ = flow rate (number of moles per unit time and unit area),
v_I, v_{II} = volumes of bulbs *I* and *II*,
R = gas constant
T = absolute temperature,
t = time.

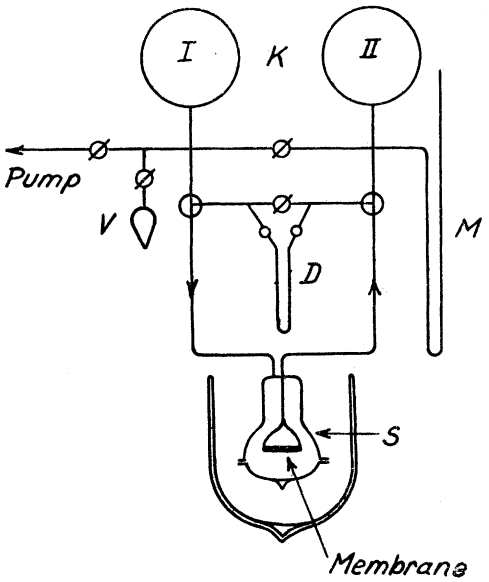

Fig. 12 — Apparatus for streaming experiments

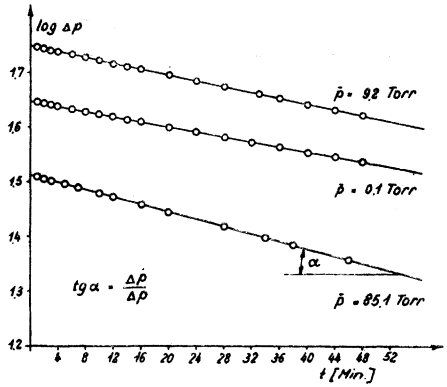

Fig. 13 — Determination of the rate of flow

Accordingly, a plot of log Δp against the time t should give a straight line, the slope of which is $\Delta\dot{p}/\Delta p$, thus allowing calculation of $\dot{n}/\Delta p$ — the number of moles (or the volume at S.T.P.) per unit time, unit pressure drop and unit area. The plot of this figure against the mean pressure $\bar{p}$ should give, according to equation (*3*), a straight line through the origin. Fig. 13 shows some plots of log $\Delta p/t$ at three pressures, Fig. 14 shows plots of $(\dot{n}/\Delta p)/\bar{p}$. It can be seen that straight lines (indicating the validity of the Poiseuille equation) are obtained above a certain pressure. At low pressures, however, the curves become horizontal, which means that the mass flow becomes independent of the pressure. This is due to the Knudsen molecular diffusion,

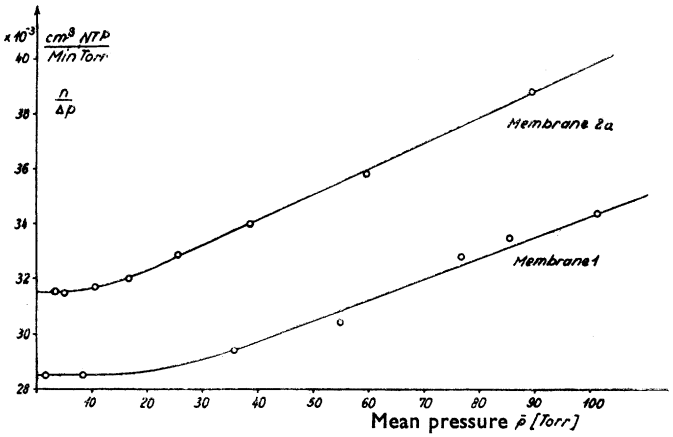

Fig. 14 — Rate of air flow through two papers at various pressures
(Torr = mm. mercury pressure at 0°C)

which occurs when the mean free path of the air molecules is of the order of magnitude of the pore diameter. In this case, the mass transfer does not take place by intercollisions of the molecules, but only by collisions with the pore walls and preferred reflection into the direction of the pressure drop. Therefore, mass transfer no longer depends on the number of molecules per unit volume — that is, on the pressure.

At 10 — 20 mm. mercury, the mean free path is of the order of 10^{-4} — 10^{-5} cm., in accordance with the order of pore radii found expermimentally (*see* Fig. 2, 5—8). A mean value of the pore radius can be obtained by comparison of the Poiseuille and the Knudsen branch of the flow rate curves in Fig. 12. For our simple pore model of a paper sheet, we can write the Poiseuille equation for an assembly of pores of different radius r and length L as follows —

$$\frac{\dot{n}_p}{\Delta p} = \frac{\pi}{8\eta} \sum_i \frac{n_i r_i^4}{L_i} \cdot \frac{\bar{p}}{RT} \qquad \ldots\ldots\ldots\ldots\ldots\ldots\ldots\ldots (5)$$

Correspondingly, the Knudsen equation has the form —

$$\frac{\dot{n}_k}{\Delta p} = \frac{4\sqrt{2\pi}}{3\sqrt{MRT}} \sum_i \frac{n_i r_i^3}{L_i} \qquad \ldots\ldots\ldots\ldots\ldots\ldots\ldots\ldots (6)$$

Combining these two equations, we can compare the slope of the Poiseuille branch in Fig. 14 with the ordinate of the horizontal Knudsen branch. Thus we obtain —

$$\bar{r} = \frac{\sum \frac{n_i r_i^4}{L_i}}{\sum \frac{n_i r_i^3}{L_i}} = \frac{32\eta}{3} \sqrt{\frac{\overline{2RT}}{\pi M}} \frac{\dot{\Delta n}_p}{\dot{n}_x \Delta \bar{p}} = \frac{16}{3} \eta \, \bar{w} \frac{\dot{\Delta n}_p}{\dot{n}_k \Delta \bar{p}} \qquad \ldots\ldots\ldots\ldots\ldots (7)$$

where M = molecular weight,

η = viscosity,

$\bar{w} = 2 \sqrt{\frac{\overline{2RT}}{\pi M}}$ = mean molecular velocity.

This, of course, is not the arithmetic mean radius, but values for various papers have again been found to lie in the order range of 10^{-4} — 10^{-5} cm.

It will be noticed in Fig. 14 that the extrapolated Poiseuille branches do not go through the origin, but meet the ordinate at a finite positive value. This is due to the slip effect that results from a deviation of the flow profile in the pores from the laminar form (discontinuity of the flow velocity at the pore walls).

Water vapour

The second case of permeation phenomena (gas interacting with cellulose) is realised by water vapour permeating through paper. It has been investigated in the same apparatus as before (Fig. 12), the only difference being that the pressure range is restricted by the saturation pressure of water vapour. This, however, is the pressure range where Knudsen diffusion and slip are the effective transfer mechanisms. As diffusion and pressure flow become identical in this case, it does not matter whether we establish a drop in partial pressure or in absolute pressure to cause permeation. Consequently, we can use the same techniques as in the air permeation experiments.

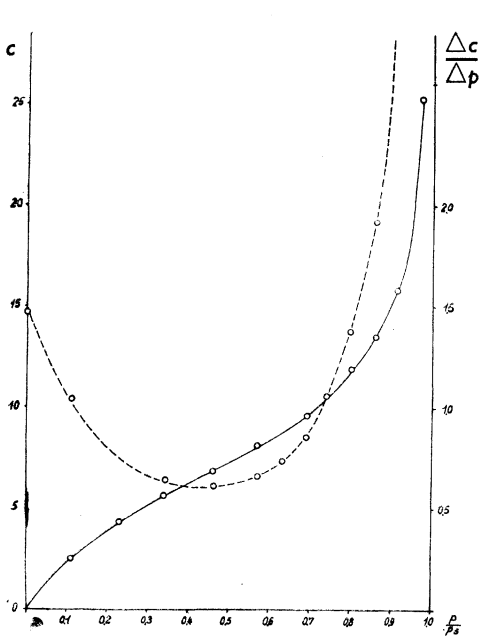

Fig. 15 — Movement of water vapour through different papers
(Torr = mm. mercury pressure at 0°C)

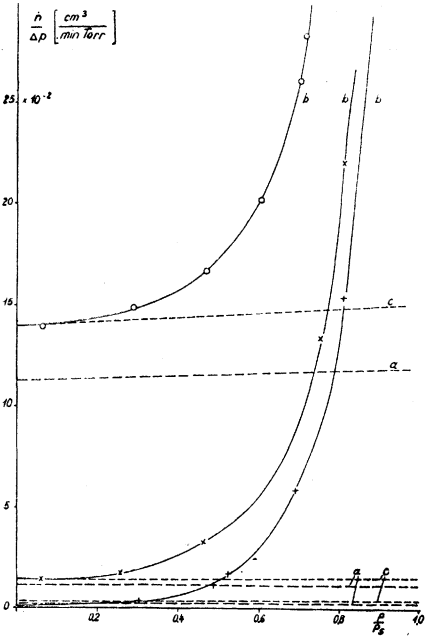

Pressure (mm. mercury at 0°C)

Fig. 16 — Adsorption isotherm of cellulose

After evacuation, a given water vapour pressure is established on both sides of the sample. After that, the pressure is increased or decreased on one side of the sheet. Pressures can easily be controlled by immersing the water containing bulb *V* (Fig. 12) in a suitable thermostatically controlled bath. Evaluation is the same as before. Fig. 15 shows three flow rate curves

at 20°C. As previously, $\dot{n}/\Delta p$ is plotted against p (curves *b*). The water vapour pressure is given as the fraction of the saturation pressure at 20°C. The dotted lines (curves *a*) give the flow rate of air. If water vapour were to behave like an inert gas, the flow rate curves would be nearly parallel to the air curves (curves *c*). They would indicate higher flow rates for water vapour than for air, because the flow rate is inversely proportional to the square root of the molecular weight — *see* equation (*6*). In fact, the curves for water vapour begin exactly at this value, but rise steeply at about 25 per cent. R.H. This additional transfer reveals the onset of a special mass transfer mechanism.

Some practical experiences also indicate a special mechanism for water vapour. Two of them may be mentioned briefly.

1. Prolonged beating of the pulp makes the paper greaseproof. The mean pore radius decreases roughly by one power of ten for the commercial range of freeness (for example, from 16° to 85° S.R.). Consequently, the air permeability decreases by 4—5 powers of ten, according to the Poiseuille equation. The water vapour permeability (WVP), however, decreases roughly by 30—40 per cent. Therefore, it is not possible to make a water vapour proof paper only by beating. This fact has created the development of laminated and other converted packaging papers.
2. Water vapour permeability is usually determined by sealing the opening of a metal box with the sample of paper. The box may contain water (100 per cent. R.H.) or a desiccant (0 per cent. R.H.) The surrounding air has standard humidity (in most of Europe, 65 per cent. R.H.). We have thus two humidity drops available — 100 — 65=35 per cent. and 65 — 0=65 per cent. In a normal diffusion process, the WVP for the 65 — 0 drop should have about double the value of the 100 — 65 WVP: however, the latter is found to be 4 — 5 times the former.

These two experiences show that —

(*a*) The flow rate of water vapour is faster, compared with air, than should be expected by the difference in molecular weight.
(*b*) The WVP is not proportional to the drop in relative humidity on both sides of the sheet.

The additional transfer of water vapour is caused, as we now know, by surface diffusion. Water vapour is strongly adsorbed by the hydroxyl groups of cellulose. The water molecules are able to jump from OH group to OH group, without leaving the surface. General movement follows the direction of the surface concentration gradient. This gradient is connected with the drop in relative humidity by the adsorption isotherm. Fig. 16 shows one example as an illustration. The circles are experimental values, the isotherm (solid curve) has been calculated according to the theory of multilayer adsorption by Brunauer, Emmett and Teller (BET), assuming six maximum layers of water. The dotted curve is the gradient dc/dp.

The characteristic and well-known shape of the adsorption isotherm explains at once the two practical experiences mentioned before —

(*1*) By beating, the pore radius is diminished, but the adsorption isotherm is practically unchanged. As the transfer of water vapour is controlled by the gradient in surface concentration, the WVP is scarcely affected by beating. Only the transfer through the pores is reduced, but this is normally only a small fraction of the whole water vapour transfer (*see* Fig. 15).

(*2*) The steep rise of the adsorption isotherm means that the gradient of the surface concentration from 100 per cent. to 65 per cent. R.H. is much greater than from 65 per cent. to 0 per cent. R.H. Therefore, the WVP is considerably larger in the former case than in the latter.

Surface diffusion can be treated according to Fick's law for normal diffusion, that is, for a single pore —

$$\dot{n} = -{}^{\circ}DU\frac{dc}{dL} \qquad \ldots\ldots\ldots\ldots\ldots\ldots\ldots\ldots\ldots\ldots \quad (8)$$

where ${}^{\circ}D$ is the surface diffusion coefficient,
U is the circumference of the pore and
dc/dL is the gradient of surface concentration across the paper sheet.

We write —

$$\frac{dc}{dL} = \frac{dc}{dp} \times \frac{\Delta p}{L},$$

thus approximating dp/dL by $\Delta p/L$, because of the low value of L. Experiments have shown that ${}^{\circ}D$ depends linearly on the surface concentration itself. Thus, we obtain for the additional transfer —

$$\left(\frac{\dot{n}}{\Delta p}\right)_{add} = const.{}^{\circ}D_o c\,\frac{dc}{dp} \qquad \ldots\ldots\ldots\ldots\ldots\ldots \quad (9)$$

In this equation, dc/dp is the slope of the adsorption isotherm.

Fig. 17 shows experimental plots of $\left(\frac{\dot{n}}{\Delta p}\right)_{add}$ against $c \cdot \frac{dc}{dp}$.

Straight lines are obtained. Their slope is a measure of the surface diffusion coefficient. The curves meet on the abscissa at a certain value of $c \cdot \frac{dc}{dp}$, which corresponds to about 25 per cent. R.H. at 20°C — that is, 4.7 per cent. water content of the paper. The BET plots of the adsorption isotherms showed that this water concentration corresponds to the amount of water covering the first layer. We may conclude, therefore, that the first layer of water molecules

is immobile. The higher layers may become more and more mobile and so explain why the surface diffusion coefficient is zero low about 25 per cent. R.H. at 20° C (Fig. 15) and is then proportional to the surface concentration — that is, to the number of adsorbed layers.

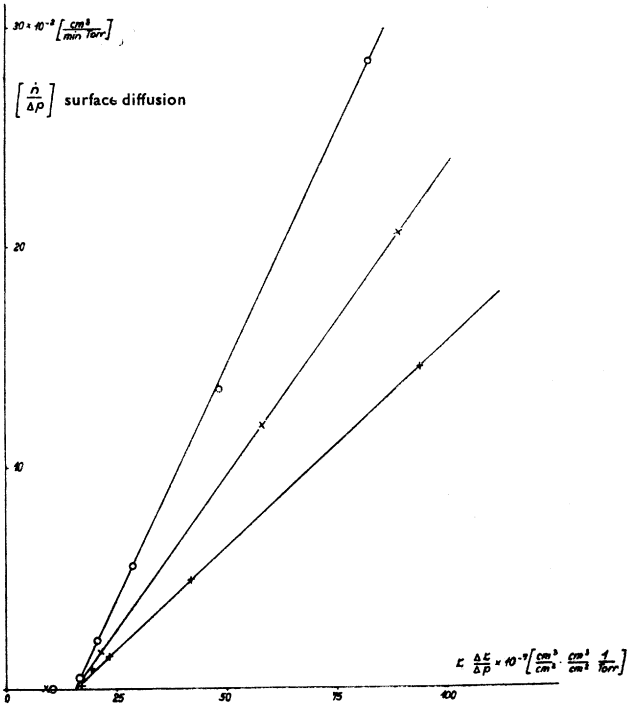

Fig. 17 — Relationship between surface diffusion and adsorption isotherm (Torr = mm. mercury pressure at 0°C)

This result enables us to determine the WVP at any drop in partial pressure (or relative humidity) by measuring the adsorption isotherm and only one rate of the WVP under suitable conditions. The former requires only two measurements, applying the BET theory. That is because one point on the straight line in Fig. 17 is sufficient to find its slope and, from that, by integration, the WVP for any given difference in relative humidity. Fig. 18 illustrates the procedure of graphical integration. It can be seen that the experimental values (circles) very well fit the calculated curve, provided the relative humidity difference is not too large. Table 2, obtained from Fig. 18,

shows that the experimental readings of the WVP agree fairly well with the calculated values.

The influence of temperature on the WVP is of special interest. We know that increasing the temperature will diminish the slope of the adsorption isotherm. This effect will lower the WVP. On the other hand, the surface

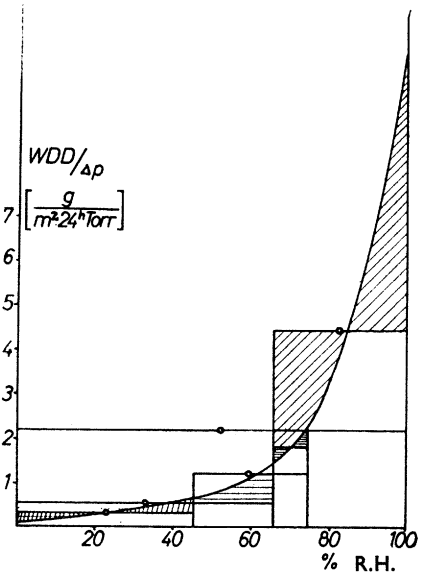

Fig. 18 — Water vapour permeability at various drops in relative humidity
(Torr = mm. mercury pressure at 0°C)

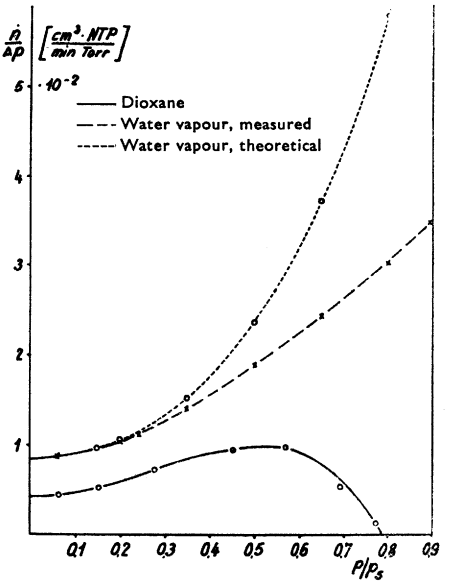

Fig. 22 — Movement of water vapour and dioxane through vegetable parchment

TABLE 2

Experimental and calculated WVP for different relative humidity drops

Difference in R.H., %	*WVP* (*g./m.²/day*)	
	Calculated	*Experimental*
0 — 45	2.10	1.85
0 — 65	4.63	4.62
45 — 75	4.38	4.45
65 — 75	3.78	3.10
65 — 100	20.1	19.4
0 — 100	24.6	24.9

diffusion coefficient will increase with increasing temperature. In order to separate these two effects, we determined the flow rates of water vapour at different temperatures and evaluated the experimental results according to the adsorption isotherms that had been found at these temperatures. Thus, the effect of temperature on adsorption was eliminated and its effect on surface diffusion was left. Fig. 19 shows some experimental results for two papers at 20°, 40° and 70°C. The slopes of the straight lines increase with increasing temperature, indicating a corresponding increase of the surface diffusion coefficient.

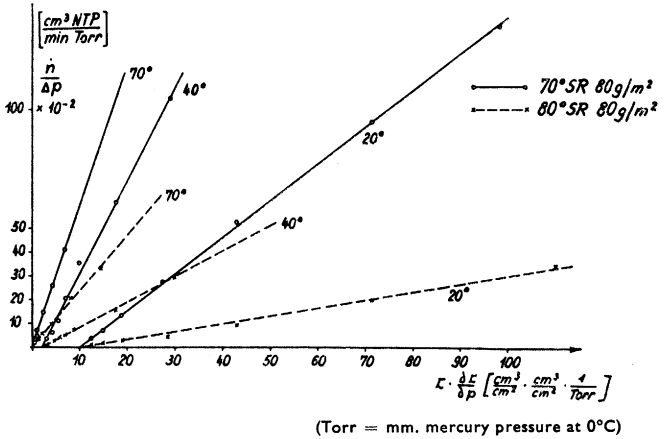

Fig. 19 — Dependence of temperature on surface diffusion

The quantitative treatment follows the Arrhenius equation —

$$^{c}D_o = const.\, exp\,(-E_A/RT) \qquad \ldots\ldots\ldots\ldots\ldots\ldots \qquad (10)$$

where E_A is the energy of activation. An average value from a number of experiments with different types of paper was 8 — 8.5 Kcal./mole. This value is quite reasonable, compared with data for other systems; similarly, the values of the surface diffusion coefficient itself, which has been found to be of the order 10^{-7} cm.²/sec., is comparable with values of other systems recorded in the literature.

In order to get the temperature dependence of $\dot{n}/\Delta p$, we must know, for equation (9), the temperature dependence of dc/dp, the slope of the adsorption isotherm. The inverse, dp/dc, depends, at constant surface concentration c, on the temperature in the same way as does the equilibrium pressure p, because a change in temperature acts like an affine transformation

of the abscissa in the adsorption isotherm. Fig. 20 shows plots of ln (dc/dp) against $1/T$ (temperature is plotted in °C). One obtains straight lines, the slope of which is proportional to the heat of adsorption. The slopes would be equal at the three concentrations, taken as parameters, if the heat of adsorption were constant for all concentrations.

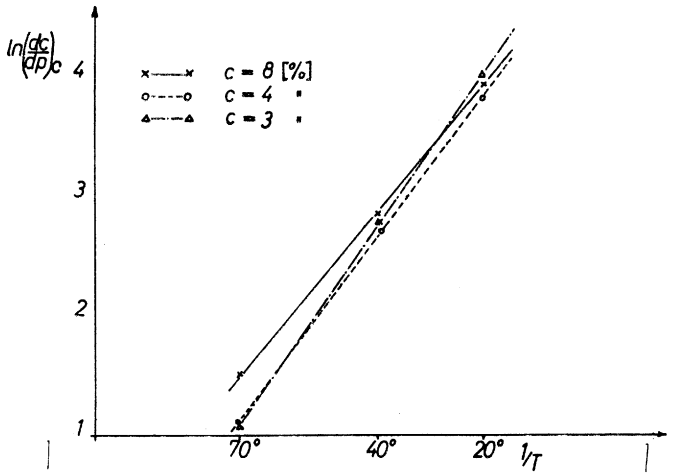

Fig. 20 — Dependence of temperature (°C) on the concentration gradient

Taking c as parameter, we can rearrange equation (*9*) —

$$\left(\frac{\dot{n}}{p}\right)_c = const.\, exp\left(\frac{E_{Ads} - E_A}{RT}\right) \quad \ldots\ldots\ldots\ldots\ldots \quad (12)$$

Now, E_{Ads} must be larger than E_A for the following reason. If E_A were larger than E_{Ads} or equal to E_{Ads}, a molecule overcoming the potential barrier given by E_A would desorbe and no surface diffusion would occur. This means that the WVP per unit pressure drop decreases with increasing temperature. This result is rather surprising. For, if we assume that the drying rate of paper above 70 — 75 per cent. solids is mainly controlled by surface diffusion, we come to the conclusion that the drying rate decreases with increasing temperature. This is true if we consider the drying rate at a given drop in absolute vapour pressure. If, however, the drying rate or the WVP is considered at a given drop in relative humidity, we have to divide Δp in equation (*12*) by the saturation pressure p_s. Hence, we obtain—

$$\left(\frac{\dot{n}}{\Delta(p/p_s)}\right)_c = const.\ exp\left(\frac{E_{Ads} - E_L - E_A}{RT}\right) \quad \ldots\ldots\ldots\ldots \quad (12a)$$

where E_L is the heat of evaporation. Now, the difference $E_{Ads} - E_L$ is always smaller than E_A. This is shown in Fig. 21, where average values are given (valid at about 20°C). Therefore, the WVP, reduced to unit relative humidity drop, increases with increasing temperature.*

For rough estimations, we can assume average values for E_{Ads} and E_A (12 — 13 Kcal./mole and 8 — 8.5 Kcal./mole, respectively). In this case, we can use equation (*12a*) to calculate the WVP for any temperature. Combined with what was said above, we need only one WVP value for a small relative humidity drop and two equilibrium moisture contents in order to get an estimation for the WVP at any climatic conditions. The reliability has been found surprisingly high compared with the error of a usual WVP determination.

In the case of very compact materials, the WVP is not only controlled by surface diffusion, but is affected by capillary condensation, too. This can be easily found in systems with minor adsorption. For instance, the WVP through polyethylene shows a maximum at about $p/p_s = 0.75$ and falls off rapidly at higher relative humidities. Probably, a considerable proportion of the very small pores is filled up with water by capillary condensation. Thus, these pores are plugged and the WVP is controlled by the rate of evaporation rather than by surface diffusion. According to the Thomson equation —

$$\ln\frac{p_s}{p} = \frac{2\sigma M}{r\varrho RT} \quad \ldots\ldots\ldots\ldots\ldots\ldots \quad (13)$$

(where ϱ = density of the liquid) the pores should be of the order 10_{i}^{-6} — 10^{-7} cm., near the limit of validity of this equation. In fact, using the dioxane method described above, the smallest pores were found to be below 10^{-6} cm.

In cellulose materials, the strong surface diffusion of water vapour through larger pores overcomes the plugging effect of capillary condensation in the smaller ones. Therefore, a maximum of permeation is only found with vapours of organic liquids showing less adsorption. Fig. 22 shows the permeation of dioxane through vegetable parchment. The maximum at about $p/p_s = 0.6$ indicates capillary condensation in pores smaller than

* A rough rule states that, for medium p/p_s values, E_A is about 0.8 E_{Ads}. This would mean that a system with a heat of adsorption more than five times the heat of evaporation would have a positive exponent in equation (*12a*) and hence a negative temperature coefficient of the WVP or the drying rate, respectively. Until now, no such system has been found.

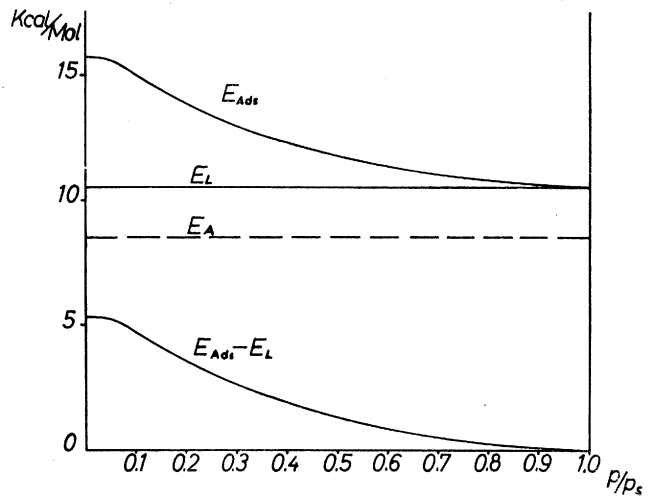

Fig. 21 — Heat of adsorption, heat of activation and heat of evaporation for various relative vapour pressures

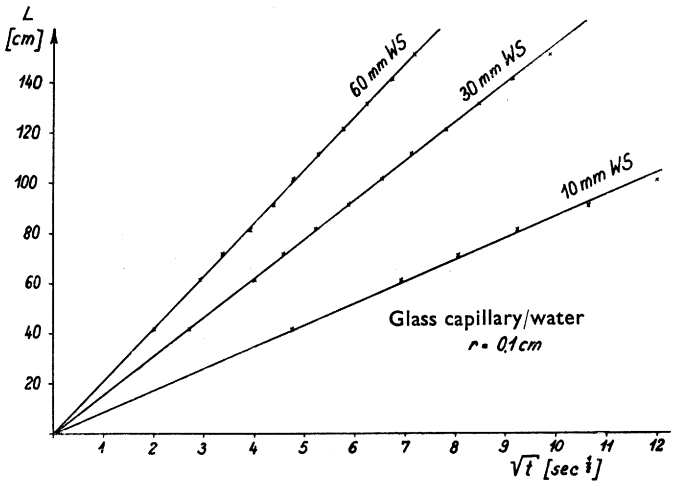

Fig. 23 — Penetration of water into a glass capillary

5×10^{-7} cm., according to equation (*13*). WVP does not show this maximum, for the reason mentioned above, but the curve is lower than that calculated from values at low relative humidity and from the adsorption isotherm. This drop of the WVP may be considered as an effect of capillary condensation in the smallest pores.

Organic liquids

The flow through paper of organic liquids, which do not cause swelling of the cellulose, may be considered as a normal Poiseuille flow similar to air permeability. It should be controlled by the viscosity of the liquids only. Table 3 shows some experimental results on a paper from unbeaten pulp.

TABLE 3

Flow rates of liquids through paper

Penetrating material	$\dot{v}/\Delta p$, *cm.³/min. cm.² mm. water*	η, *cp*	$\eta.\dot{v}/\Delta p$, $\times 10^2$
Air	0.91	0.0181	1.64
Acetone	4.93×10^{-2}	0.322	1.59
Toluene	2.65×10^{-2}	0.586	1.58
Dioxane	1.21×10^{-2}	1.26	1.53
n-Butyl alcohol	5.20×10^{-3}	2.95	1.53
iso-Butyl alcohol	3.91×10^{-3}	3.95	1.54

Actually, the product $\eta.\dot{v}/\Delta p$ is nearly constant. It seems to decrease slightly with increasing viscosity. Perhaps the heavier liquids cannot penetrate all the pores accessible for air.

The steady flow of such liquids through paper is not very interesting. In most practical cases, the initial period of the steady flow (that is, the penetration period) is of more importance. An additional effect coming into account here is the interface tension or the heat of wetting of the penetrating liquid against the pore material.

The time law of penetration can be demonstrated by a simple experiment. Water is forced under a slight pressure into a horizontal glass capillary tube. The volume rate of flow is determined by the hydrostatic pressure p and the capillary pressure $2\beta/r$, where $\beta = \sigma \cos \theta$ is the interface tension. So we have —

$$dv = r^2\pi\, dL = \frac{\pi r^4}{8\eta L}\left(p + \frac{2\beta}{r}\right) dt$$

or

$$LdL = \frac{r^2}{8\eta}\left(p + \frac{2\beta}{r}\right) dt,$$

which when integrated gives — $L = const. \sqrt{t}$ ..... (*14*)

Fig. 23 shows the validity of equation (*14*) for a single glass capillary tube, though this is also valid for porous systems. Another model experiment with a plug of clay and water as penetrating material is shown in Fig. 24. A water column is driven by constant hydrostatic pressure against the plug and, in this way, air is forced through the plug at constant speed, measured by the movement of a water droplet in a horizontal tube. When

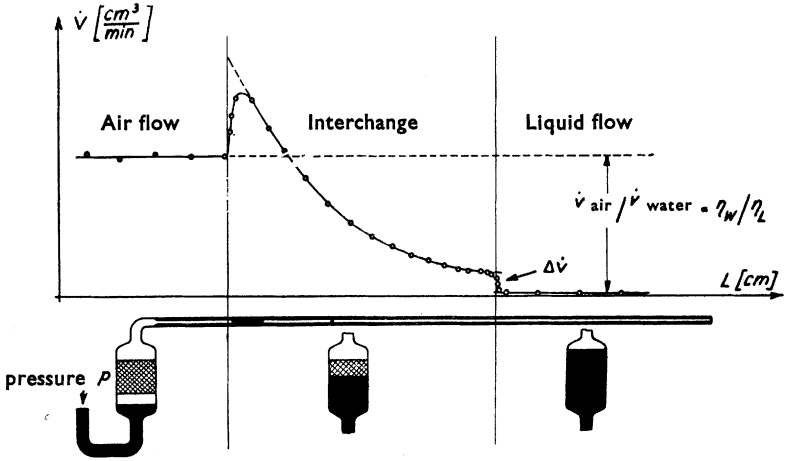

Fig. 24 — Penetration and permeation — system clay/water

the water contacts the plug, the additional capillary pressure accelerates the movement at first, but the rate of flow decreases according to equation (*14*) until the water has completely filled the plug. After that, movement is constant again, the velocity having been reduced suddenly by the absence of capillary pressure.

The volume rate of flow during the penetration period is given approximately from equation (*14*) by —

$$\dot{v} = \frac{\bar{r}^3\pi}{2}\sqrt{\left(\frac{p+2\beta/\bar{r}}{\eta}\right)}\cdot\sqrt{t} \quad \ldots\ldots\ldots\ldots\ldots \quad (14a)$$

Immediately before the end of penetration, it becomes —

$$\dot{v} = \frac{\pi}{8\eta}\left(p + \frac{2\beta}{\bar{r}}\right) \sum \frac{n_i r_i^4}{L_i}$$

The steady flow rate after penetration is given by —

$$\dot{v} = \frac{\pi}{8\eta} p \sum \frac{n_i r_i^4}{L_i} .$$

Thus, the drop in flow rate at the end of penetration (Fig. 24) is given by —

$$\Delta\dot{v} = \frac{\pi\beta}{4\eta\bar{r}} \sum\left(\frac{n_i r_i^4}{L_i}\right) = \textit{approximately } \frac{\pi\beta\bar{r}^3}{4\eta L} \quad \ldots\ldots\ldots\ldots \quad (15)$$

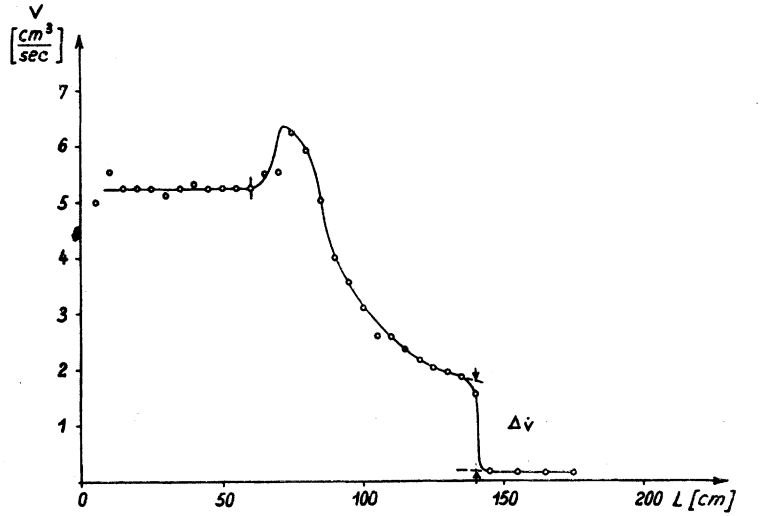

Fig. 25 — Penetration and permeation — system cellulose/benzene

From equations (*14a*) and (*15*), $\bar{r}^3$ and β may be calculated and so offers the possibility of calculating approximately the interface tension of a liquid in a porous material. Fig. 25 shows the experimental curve, corresponding to Fig. 24, of benzene penetrating into a plug of cellulose. The value found for the interface tension was 40 dynes/cm.

It is well known that paper behaves according to equation (*14*), but no values seem to have been worked out from equations (*14a*) and (*15*) for the determination of the interface tension β. This could be interesting in order

to explain the different penetration rates of printing inks having the same viscosity.

A problem of special interest in paper testing is to combine the penetration of inert liquids with air permeability. This has been considered with special regard to grease resistance. Taking a single capillary tube, we obtain for the leak time, t^* (the time from the beginning to the end of penetration, the middle section in Fig. 24) from equation (*14*) the expression —

$$t^* = \frac{4L^2\eta}{r^2\,(p+2\,\beta/r)} \qquad \ldots\ldots\ldots\ldots\ldots\ldots\ldots \qquad (16)$$

We can distinguish two limiting cases —

(*1*) When r is large — $2\,\beta/r \ll p \rightarrow t^* = \dfrac{const.}{r^2\,p}$ ..... (*16a*)

(*2*) When r is small — $2\,\beta/r \gg p \rightarrow t^* = \dfrac{const.}{r\,\beta}$ ..... (*16b*)

The steady volume rate of air flow at a given pressure drop, $\dot{v}$, is proportional to r^4. Thus, we have for the two limiting cases —

(*1*) $t^* = const.\,\dot{v}^{-1}\,.\,p^{-1}$ or $\log t^* = const. - \frac{1}{2}\log \dot{v} - \log p$ ..... (*16c*)

(*2*) $t^* = const.\,\dot{v}^{-1}\,.\,\beta^{-1}$ or $\log t^* = const. - \frac{1}{4}\log \dot{v} - \log \beta$ ..... (*16d*)

It is of some interest to examine this simple alternative immediately with paper. Fig. 26 shows plots of $\log t^*/\log \dot{v}$ from experimental results on some greaseproof and glassine papers, using pork lard for the grease resistance test and applying the two hydrostatic pressures 4 g./cm.^{2} (circles) and 20 g./cm.^{2} (crosses and triangles). The least squares straight lines have the slope $-\frac{1}{2}$, thus confirming equation (*16c*). It will be noticed that the distance between the two lines is $\log (20/4) = 0.7$ on the logarithmic scale as required by equation (*16c*).

It is remarkable that the relationship between the leak time and the steady flow rate, as derived for a single capillary, is also valid, at least in principle, for a paper sheet. There is one striking difference between these two systems, however: in a capillary, t^* and $\dot{v}$ refer to the same opening, whereas, in a sheet of paper, $\dot{v}$ is a property of all pores passed by air, while t^* is a property of the largest pores only, for the leak time is here defined by the time when the first spots of grease appear on the back of the sheet. This, of course, will occur through the largest pores. It is a consequence of the

general character of the pore size distribution, set out in Fig. 11, that the frequency of a certain large pore size is closely related to the whole shape of the distribution curve, to $\bar{r}$ and r^4, controlling air permeability. Alternatively, we can say that the average radius of the largest 1 or 2 per cent. of all pores is strongly related to the average or the fourth moment of all pores. A rigorous statistical treatment of distributions, averages and moments, instead of single pores, leads to the result that the slope of the log/log curve from equation (*16c*) is not —0.5, but about —0.6. This has been found to be true by examining a larger number of samples, covering a range of nearly six powers of ten in the air permeability.

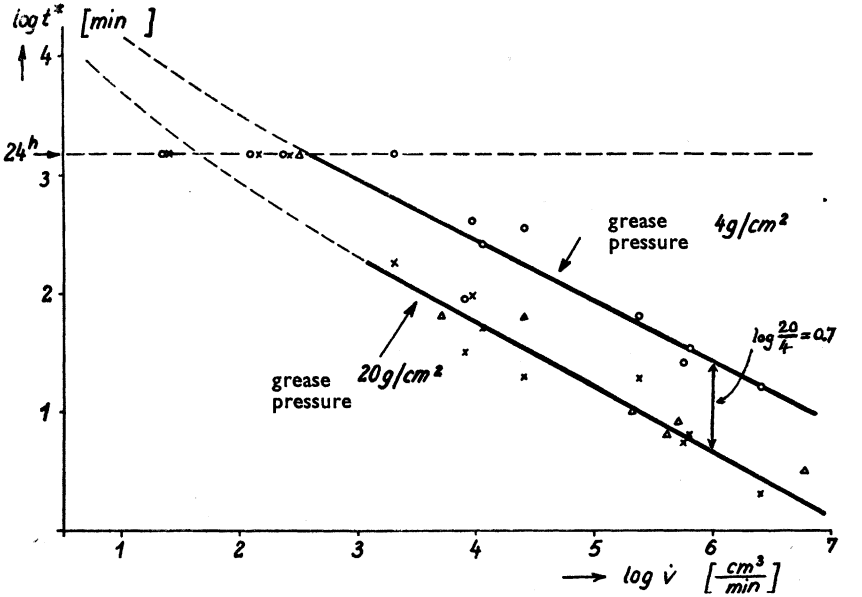

Fig. 26 — Comparison of grease resistance and air permeability (10 – log $\dot{v}$ plotted)

Fig. 27 shows a log t^*/log $\dot{v}$ graph for a number of greaseproof papers (×), glassines (○) and vegetable parchments (●). It will be noticed that most of the vegetable parchment samples lie above the straight line, which has been derived from the greaseproof and glassine papers only. This is due to the pinholes existent in vegetable parchment as mentioned earlier (*see* Fig. 7); as the air permeability is affected by their fourth power, but the leak time by this second power only. The other points also are scattered considerably round the straight line, however and is obviously a consequence of the fact

that the frequency of the largest pores (the ordinate of the far right end of the pore size distribution curve) has a large standard error from sample to sample. This is also known from the grease resistance test. The standard deviation will increase with decreasing average pore radius (towards the left end of Fig. 27). It may be expected that the points would fit the theoretical line better when they represent averages of a large number of samples.

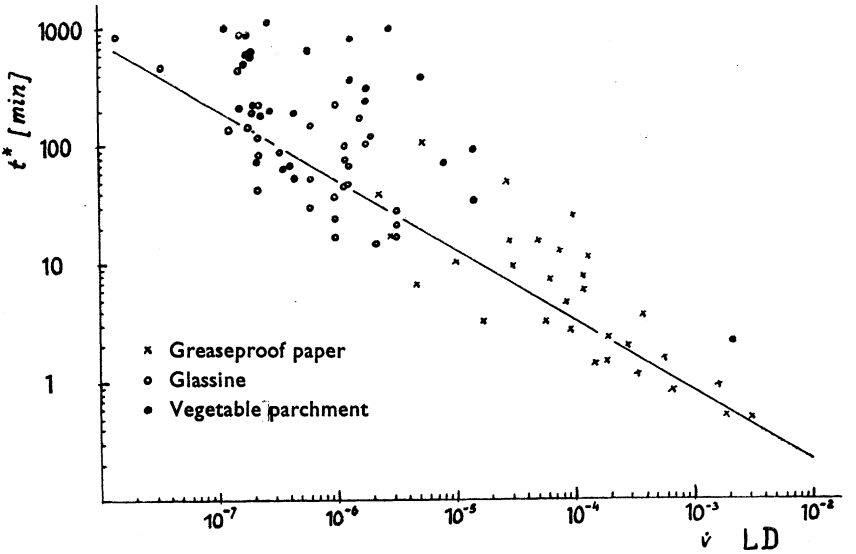

Fig. 27 — Comparison of grease resistance and air permeability

In any case, air permeability is felt to be a suitable measure of grease resistance. It may be even better than the grease resistance test itself, because it avoids long testing times for very greaseproof materials and is based on the average behaviour of paper, giving results that would otherwise be obtained only by a large number of samples. Moreover, for printing papers, air permeability is possibly of more interest than is recognised today.

Summarising all these results, we can say that the consequent use of the simple Poiseuille pore model permits the various porosity phenomena to be reduced to a small number of well-known physical laws. Of course, it is possible to use another model or to transform all equations in question into the Kozeny-Carman form or another one. As long as the model does not lead to contradictions and is used only as a guide and not as a reality, however, this seems to be of less importance than to find the physical principles of transfer and interaction that are effective in a particular case.

It will be a matter for further research to cover the last group of porosity phenomena, that is, the penetration and permeation of interacting liquids (such as water). This case seems not yet to have been treated in this way. Here, the essential feature will be the treatment of swelling, which did not need to be considered in this paper.

DISCUSSION

DR. J. A. VAN DEN AKKER: In my opinion, the work of Mr. Nordman and Dr. Gustafsson and their colleagues during the last several years has been outstandingly good and of great significance, certainly of interest to everyone working in the field of mechanical properties. Of great significance, because, until we know the importance of interfibre bonding and the breaking of bonds between fibres, we cannot even begin to create a theory concerning the mechanical properties of paper.

Mr. Nordman, I think, has used the breaking of bonds in a rather general sense, but my feeling is that the specific reference was to the breaking of bonds between the fibres. From our point of view, there are various interpretations that can be placed on observations of the sort Mr. Nordman has presented to us today and published with his associates in the past. The first is that there can be interfibre bond breaking. The second, a suggestion made by Dr. Valley of the Eastman Kodak Co. in Rochester, is the possibility that, as a sheet is stressed, unbonded fibre elements that happen to be close enough to each other to give rise to what we call optical contact may be further separated, thus causing an increment in the scattering coefficient. Incidentally, we have some information to the effect that the thickness of a sheet increases rather than decreases when the sheet is stressed. This could be a sign of bond breaking between the fibres; also of simple separation between the fibres without the breaking of bonds.

The third possibility is that the individual fibres exhibit an increase in light scattering when stressed. We do not yet have much evidence for this. During his thesis work, Howard Leech made the interesting observation that fibres dried by the solvent exchange process scattered much more light (magnification $\times$ 200 with dark field illumination) than water-dried fibres. This shows that the expanded system of a fibre can scatter light, presumably because of the rupture of intrafibre bonds. Now, when a fibre is stressed, we may open up the structure of the fibre sufficiently to cause some change in the amount of light scattered by the fibre. I think that, tentatively, we have to admit all these possibilities; then it is just a question of the relative importance of the several mechanisms in particular cases. Obviously, if one has a poorly bonded sheet, there will be extensive bond breaking. If one is dealing with a sheet prepared from well-beaten pulp, the amount of interfibre bond breaking would be much less and possibly the amount of intrafibre bond breaking much more.

We are at present working on the scattering of light from individual fibres that are under stress, but do not have enough data yet to report. It has been quite a job, as you might imagine, to arrange apparatus sufficiently steady and sensitive to do this. This involves a photomultiplier tube and an optical system that enables one to see where the fibre is in relation to the zone of illumination. In our earlier apparatus, the fibre moved relatively to the illuminated zone and we got changes in the amount of light scattered that were clearly spurious. We hope to complete these and other refinements and be in a position in another year or so to report some data.

MR. J. BOS: In Mr. Nordman's paper is given a detailed survey of the significance of the scattering coefficient of normal and butanol-formed sheets for the determination of the unbonded and the total surface of fibres in paper. He mentioned also uncertainties involved in the underlying assumptions, especially raised by the work of Haselton.

Recently, we experimented with butanol sheets and this may give further justification of and reasons for the correction factor applied on the *s* values of butanol sheets by Haselton, Leech and Nordman.

The experiments were performed on a bleached softwood sulphate pulp, beaten to 26° S.R. The scattering coefficient of the normal sheets is 210 cm.²/g.; for the butanol sheets it is 930 cm.²/g. We calendered the butanol sheets in a laboratory calender and to our surprise the *s* value decreased considerably, depending on the pressure applied, until a value of 400 cm.²/g. was reached. Calendering of the normal sheets gave only an insignificant fall in scattering coefficient, down to 200 cm.²/g.

Influence of calendering on sheets formed in different media

Medium	*Scattering coefficient, cm.²/g.*		*Burst factor*		*Relative pressure applied in calendering*
	O	*C*	*O*	*C*	
Water	210	200	48	50	1
Acetone/water (1 : 1)	270	250	37	42	1
Acetone/water (3 : 1)	370	350	21	22	1
Butanol	930	400	(6)	12	1
		470		11.5	$\frac{3}{4}$
		690		8.5	$\frac{1}{2}$
		780		7.5	$\frac{1}{4}$

O = original *C* = calendered

The explanation of this decrease in the *s* value of the butanol sheets could, to our knowledge, only be that the bonded surface area of the fibres had increased considerably and, therefore, also the strength of the sheets.

Determination of the bursting strength gave the values in the following table. The decrease in scattering coefficient of the butanol sheets through calendering is not accompanied by a corresponding increase in bursting strength.

To get some intermediate values, we made sheets in acetone/water mixtures (1 : 1 and 3 : 1). With these sheets, there is only the same slight effect of the calendering on the values of the scattering coefficient and the burst factor (*see* table opposite).

By plotting the scattering coefficient against the burst factor, all measurements (except those made on the original butanol sheets) fall on a straight line, which gives the real change in bonded surface area with strength. Through extrapolation to zero burst factor, we get about 500 cm.²/g. for the *s* value of the unbonded sheets (*see* Fig. **R**). The *s* value of the butanol sheets was 930 cm.²/g. The ratio of these two values is again this correction factor, in this case 0.55, which is about the same as that given by Haselton and Leech. More experiments should be performed to obtain a reliable value.

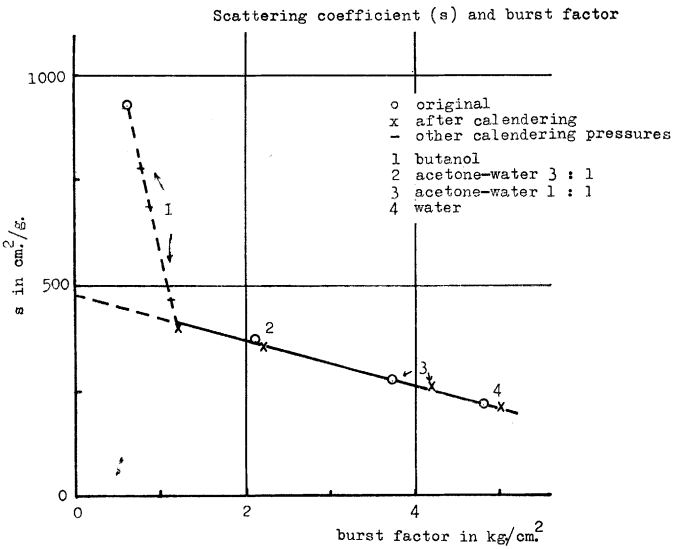

Fig. R

One thing has still to be explained — what is happening in calendering a butanol sheet. Here, water again comes into play — a substance we always need in our bondmaking activities. Evidence of this was obtained from our last experiment. We dried regular butanol sheets in an ordinary drying oven at 100°C and calendered the sheets immediately on leaving the oven. Now the scattering coefficient decreased only to about 650 cm.²/g. and the burst factor increased to 8.

Our conclusions on this subject are that the correction factor, first applied by Haselton and later by Leech and Nordman, is no longer a suspect figure to multiply the *s* values of butanol sheets. In calendering butanol sheets, the amount of water present in the air-dry condition is sufficient to close the light-scattering surfaces produced by internal fibrillation. These surfaces do not contribute to paper strength.

MR. L. NORDMAN: I think this is perhaps a very good explanation. The butanol sheets are very porous in structure and very heterogeneous. We have, in some other cases, observed that when we compress such a sheet (putting the same material in a smaller volume), then the scattering coefficient can change, even if nothing else happens to the structure. For instance, we have observed this, even for water-dried sheets, provided the pulp is unbeaten and very weak (for example, an unbleached aspen sulphite pulp). There was first a slight increase in the scattering coefficient upon calendering; after that, a decrease without changing the other properties of the sheet at all.

MR. O. ANDERSSON: What we have here, including Mr. Nordman's paper, will convince us that measurement of light scattering is a good tool for understanding something about the internal structure of an assemblage of cellulose fibres.

In this paper, I have found quite a few so-called Brask scraps. The author states that the evidence in favour of the light scattering coefficient being a measure of the unbonded area is only circumstantial. I would like to call it ambiguous, although it is not easy either to prove or disprove the statement. What is critical in changing the light scattering properties is the intrafacial distance. The critical distance will have an order of half or quarter of a light wavelength. As soon as an intrafacial distance passes this critical value, a change in light scattering will occur. Now, this distance is of the order 1 000 — 2 000 Å, but the critical distance in forming hydrogen bonds (which I think we will agree is the pertinent type of bond here) is of the order of $\frac{1}{100}$ — $\frac{1}{500}$ of that. That there is a change in light scattering — that is, an intrafacial distance passes its critical value — does not necessarily

mean that a bond is broken. The two occurrences might, of course, be proportional to one another.

In considering the diagrams that are put forward here, I have tried to find out whether I could become convinced that the change in light scattering during straining is proportional to strain or to energy. If we compare Fig. 4 and 7, we have the relationship between scattering coefficient and energy lost. In one case, scattering is plotted against energy and, in the other case, against strain. To me, the comparison of these two pictures is by no means exclusive on the question of linearity with energy or strain.

Fig. 2 also relates scattering to strain. This certainly does not suggest a linear relationship between the two quantities at a first glance, but, if we disregard all contraction branches and only consider the main strain branches, I think the linear approach is justifiable.

We must remember that, as soon as we commence cycling, relaxation phenomena, time delay functions, etc. will occur in the structure. These might well explain the deviation of the general linear relationship between strain and optical properties. The author has obtained a straight line by plotting energy instead of strain; but, in Fig. 3, the first branch suggests a fairly linear relationship between light scattering and strain. On the right, where the horizontal axis represents time — this is a relaxation procedure — there is a change in light scattering, although no energy change in the previous sense is involved, because of constant strain.

I would also like to comment on the agreement between measurements of the number of bonds per unit volume according to the theory put forward by Nissan and according to the present light scattering hypothesis. The agreement shown in Fig. 9 is far too good to be true, especially when considering all the hypothetical assumptions made. The Nissan theory implies that the bond density is proportional to the third power of the elastic modulus. If the method of calculation described in the present paper is written mathematically in terms of the variables involved and these variables are expressed in terms of elastic modulus, the result is a third power law of elastic modulus. The agreement may therefore only be ostensible.

MR. NORDMAN: I will answer the last question first. I have never tried to relate quantitatively the increasing scattering to anything but energy. The fact that I have produced curves showing the qualitative relationship between scattering and strain is because the experimental design could not give the energy value: I only got the scattering as a function of the strain.

In that connection, I should answer also the question about Fig. 3. There are no missing points, because there are no points; it is a curve obtained on a recorder.

I think I have already answered the question about Fig. 4 and 7. Their relationship is between scattering and energy, not between scattering and strain. The fact that we have produced curves relating scattering to strain is merely because we could follow the increasing scattering as a function of time with our recorder.

In Fig. 2, we have again produced the same type of curve. In this case, too, I believe the increasing scattering is related to the energy and not to the strain.

MR. C. R. G. MAYNARD: Work started sometime ago in our Glory Mill laboratory and carried on in one of our other laboratories may be of interest in connection with Fig. 5 and 6 in Mr. Nordman's paper. It concerns the variation in opacity produced along a strip when the strip is under strain. If a strip of transparent paper (or opaque paper that has been transparentised with a solvent or wax) is strained, two systems of opaque parallel lines that form a criss-cross pattern appear. The angles between the two systems and the strip direction depend on the angle of the strip to the grain of the paper and the type of paper. We believe that these lines are caused by higher strains occurring at these opaque parts.

A weak spot in the material causes strains beyond the 'yield point' and consequent opacity from bond breaking. The strain occurs in a line across the strip and the angle of this line is determined by the mechanical constants of the material. The severity of this opacifying effect varies over the strip and increases first in one place and then in another. This would seem to have some bearing on Fig. 6.

MR. NORDMAN: I have no comments, Mr. Chairman.

DR. I. JULLANDER: In Fig. 8 of his paper, Mr. Nordman shows that there is a difference between hardwood and softwood pulps in the relationship of bond strength and pentosan content. Which types of hardwood pulps are represented in the diagram?

I do not think the difference in specific bond strength between softwoods and hardwoods must necessarily be explained as a consequence of the chemical composition of the hemicelluloses. In paper manufacture, different carbohydrates and carbohydrate derivatives can often replace each other. It is, for instance, known that starch and carboxymethylcellulose can both be used in the manufacture of coated paper by means of a size press. The

difference in chemical structure between starch and carboxymethylcellulose must be much larger than can be expected between two types of hemicellulose.

Recalling Dr. Lange's paper yesterday, there is another possible explanation. At the same average hemicellulose (pentosan) content, the distribution across the secondary wall might be different for softwoods and hardwoods. There is no proof for this assumption in Dr. Lange's paper, however: it seems to me that his studies show us the only way to connect physics and chemistry in the study of fibre bonding in paper. I would like to ask if we can expect more results along these lines either from Dr. Lange himself or from somebody else who has taken up this type of research.

DR. P. W. LANGE: In answer to Dr. Jullander, most of my earlier work was done on spruce and, since during that time we had difficulty in collecting a sufficient amount of data, I have no detailed information about the hemicellulose distribution in different types of birch pulp. Therefore, it is not so easy to compare the two types, birch and spruce. In addition, absolute distribution curves for pulps of different wood origin are very difficult to compare, but I have a feeling that on the surface of birch fibres there is relatively more hemicellulose than on the surface of spruce fibres. Concerning the future, I hope that, with the new type of interference microscopy and with new data-collecting methods, I will be able to answer your question better the next time you ask it.

MR. NORDMAN: The woodpulps we used are all commercial pulps and, among the hardwood pulps, we used aspen pulp and birch pulp. The pulps are sulphite or sulphate or unbleached. That proves that the material is not very homogeneous and other effects can, of course, be possible.

DR. VAN DEN AKKER: In Mr. Andersson's criticism connected with Fig. 3 of Mr. Nordman's paper, he pointed out that for the relaxation portion of the figure there was no energy expenditure. This is true, there is no energy expended by the apparatus; however, if I understand the experiment, the strip of paper possessed strain energy at zero time and it seems to me quite likely that some of the strain energy was transferred to bond breaking — if, indeed, there was bond breaking in the process. In other words, I do not think we can necessarily conclude that there is a mystery about this part of the figure.

MR. NORDMAN: That is so.

DR. F. MULLER: I should like to say something about the question already touched upon by Dr. Jullander.

Mr. Nordman states in his paper (page 343) —

> "The bond strengths of hardwood pulps and softwood pulps, however, form different curves as a function of the pentosan content, the hardwood pulps forming a group below that of the softwood pulps. The results indicate that increasing amounts of hemicellulose increase the strength of the bonds, but that hemicelluloses in hardwood pulp are not as effective as are the same quantities of hemicellulose in softwood pulp."

I should like to point out that pentosans constitute the majority of the hemicellulose in hardwood pulps; they constitute less than half in softwood pulps. It is clear to me that, when you correlate bond strength with pentosan content, you get a different curve with softwood pulps than with hardwood pulps. The bulk of the hemicellulose in softwoods consists of glucomannan, which will contribute equally or even more than pentosan to bond strength.

PROF. H. W. GIERTZ: The discussion of Mr. Nordman's paper has brought out the very important question of the correlation between paper strength and opacity. Every maker of fine paper has been forced to realise that any way of increasing strength involves a reduction in opacity at the same time.

When saying strength, I mean fibre-to-fibre bonds, which, in my opinion, are best measured by tensile or bursting strengths. To increase such strength,

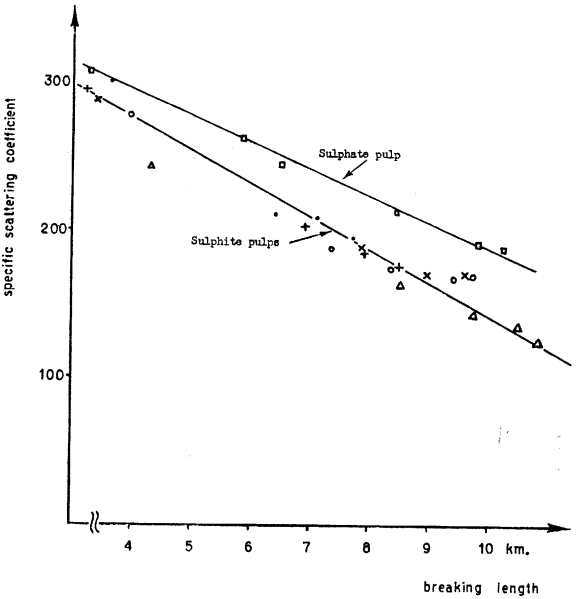

Fig. S — The relationship between specific scattering coefficient (opacity) and breaking length

we have to create contacts between the fibres and, in doing so, we lose the optical surfaces that scatter the light, thus decreasing opacity.

This correlation between breaking length (obtained by beating) and opacity (the specific scattering coefficient, *s*) is shown in Fig. S for different sulphite pulps and one sulphate pulp, all bleached and prepared from spruce. The sulphite pulps are of quite different quality, ranging from extra strong pulps (yield 55 per cent.) through ordinary pulps to rayon grade pulps and one extra soft pulp (yield 39 per cent.) Nevertheless, there is a very close relationship between strength and opacity: the coefficient of correlation is 0.99. The same relationship holds for the sulphate pulp, though the opacity in this case is on a higher level and the drop in opacity is not so serious. For the sulphite pulps, an increase of 1 000 m. in the breaking length corresponds to a decrease of 30 units in the *s* value; for the sulphate pulp, however, this decrease is only 21 units. Obviously, when trying to combine strength with opacity, it is better to use bleached sulphate pulps than sulphite pulps.

THE CHAIRMAN: I have felt for a long time that this work by our Finnish colleagues, however controversial it may be, is one of the most significant lines of work that has been carried out for many years and the discussion this afternoon has shown that other people may have that point of view, even if they disagree with the particular interpretations that have been put forward.

MR. D. S. BELFORD: I was very interested to hear Prof. Centola's references to the action of aqueous solutions of various salts on cellulose fibres. In the Biophysics Department at Leeds University, we have recently been carrying out some work on the location of water soluble preservatives introduced into timber by pressure treatments. During this work, we have used the technique of transmission electron diffraction in the electron microscope. We have, for instance, treated Douglas fir shavings with an aqueous 4 per cent. copper sulphate solution, allowed them to dry at room temperature and subsequently blended them for examination in the electron microscope.

Untreated wood particles do not give an electron diffraction diagram of cellulose under these conditions, because of the relatively low lattice perfection of the crystalline component of wood cellulose mentioned earlier by Dr. Rånby. Certain particles from the copper sulphate treated wood, on the other hand, give quite characteristic oriented electron diffraction diagrams.

The spacings calculated from the electron diffraction diagram oriented with respect to the direction of the cellulose microfibrils do not correspond with any known copper salt listed in the ASTM Crystallographic Index.

Similar patterns were obtained from cotton cellulose and from wood treated with aqueous solutions of zinc sulphate, ferric sulphate, cobalt sulphate and potassium dichromate. The pattern shows a tendency to fade, owing to the effects of the electron beam, which is fairly characteristic of organic rather than of inorganic substances.

I would emphasise here that we have so far been working with this material purely from the point of view of preserving wood and not from a fundamental point of view.

More work is needed before a clear explanation of these results can be made, but we suggest that the electron diffraction diagram may be given by a metallo-cellulose complex. It is inconceivable that any modification takes place of the crystalline component of cellulose, since water is known not to penetrate within these regions and the X-ray diffraction diagram remains unchanged after treatment. It may be that the copper, for example, is involved in a cross-linking between adjacent cellulose molecules in those amorphous regions of the microfibril where the molecules of cellulose are parallel, but not evenly spaced. This is supported, to some extent, by the fact that we have been unable to detect the complex in *Valonia* cellulose.

I am not suggesting that this sort of thing takes place on a large scale, since this work is not quantitative and is still in the preliminary stages. It may suggest, however, that there may be a specific action under certain conditions between aqueous solutions of various salts, on the one hand and wood fibres, on the other. At present, we have insufficient evidence to be too definite about the mechanism of the process, but I thought this work might be of general interest.

Whether these remarks have any significance in connection with the beating rate is, of course, another matter.

DR. JULLANDER: Some years ago, we made experiments having a bearing on what Prof. Centola and his co-workers have told us today. In their first investigations, published 1940, a thickening effect was observed upon addition of some substantive dyes to methylcellulose solutions. We have followed up this idea by investigating the thickening effect on aqueous ethylhydroxyethylcellulose solutions of different types of substantive dyes. More than 50 different dyes were tested, only comparatively few of them gave a positive effect. The dyestuffs with known structure giving a thickening effect all had two azo groups and at least two sulphonic acid groups. From this and from spectrophotometric studies, we have concluded that the thickening is the result of a loose cross-linking between the macromolecules by means of the dyestuff molecules.

Third discussion

I should like to ask if any investigations have been made of the constitution of those dyestuffs that are able to give the effect in the beating process just described. It could be that cross-linking effects in this case are quite unnecessary or even unwanted and, consequently, the requirements on the constitution of the dyestuff different

PROF. G. CENTOLA: In the second table of our paper, we have presented the effect of many dyes on beating and we have seen that Congo Red (the molecule has two sulphonic acid groups) was the most active among them. Many years ago, I observed a similar trend when I measured the changes of specific viscosity for a methylcellulose following addition of a series of substantive dyes to its water solutions. The maximum increase of specific viscosity of the methylcellulose solutions was caused by those dyes that have on the one side of the molecule amino groups symmetrically distributed and on the other side some lyophilic groups, as is the case for Congo Red and Benzopurpurine. Less activity was observed for the dyestuffs that have either more than two sulphonic acid groups present in the molecule or hydroxyl groups instead of amino groups or an asymmetrical distribution of the hydroxyl, amino and sulphonic acid groups in the molecule.